Fibers and Polymers 2022, Vol.23, No.8, 2114-2122
DOI 10.1007/s12221-022-4032-4

ISSN 1229-9197 (print version)
ISSN 1875-0052 (electronic version)

Design, Synthesis, and Antibacterial Activity of Spiropyrimidinone Derivatives Incorporated Azo Sulfonamide Chromophore for Polyester Printing Application

Sherif S. Ragab[1]*, Ayman M. K. Sweed[2], Zeinab K. Hamza[3], Elkhabiry Shaban[4]*, and Ahmed A. El-Sayed[1]

[1]*Photochemistry Department, Chemical Industries Research Institute, National Research Centre, Dokki, Giza 12622, Egypt*
[2]*Chemistry of Natural and Microbial Products Department, Pharmaceutical and Drug Industries Institute, National Research Centre, Giza 12622, Egypt*
[3]*Food Toxicology and Contaminants Department, National Research Centre, Dokki, Giza 12622, Egypt*
[4]*Dyeing, Printing and Textile Auxiliaries Department, Textile Research Institute, National Research Centre, Dokki, Giza 12622, Egypt*

(Received September 29, 2021; Revised January 27, 2022; Accepted February 6, 2022)

Abstract: We designed and developed a novel series of bioactive disperse dyes by conjugation of spirocyclic 2-thiopyrimidine scaffold with aryl or sulfa drug moieties in the same construct through azo linker to take advantage of the bioactive character of both motifs. The target molecules were simply approached on a gram scale via the diazocoupling of spirocyclic 2-thiouracil **1** with aryl diazonium chloride derivatives to afford the heterocyclic azo-disperse dyes **4a-e** in excellent yield. These azo dyes were effectively utilized to make pastes for silkscreen printing of polyester fabrics. The color characteristics of the dyes and their fastness properties including washing, rubbing, perspiration, sublimation, and light fastness were also investigated. The antimicrobial activity of the produced dyes **4a-e** was evaluated against some Gram-positive and Gram-negative bacteria, and the results revealed that **4d** was more active than the standard drug cefoperazone against the Gram-positive bacteria *S. aureus*. The antibacterial efficacy of the treated fabrics has also been investigated revealing that the dyed fabric **4b** was found to have a potent inhibition on *B. cereus* (93 %), and against *E. coli* with a reduction of (90 %).

Keywords: Spiropyrimidine, Azo-disperse dyes, Sulfonamide, Polyester printing, Antibacterial

Introduction

Azo dye compounds have emerged intensively and witnessed exponential growth in the coloring industry. They contribute to at least 66 % of all colorants for textile products due to their excellent color brightness [1]. They also occupy higher chromophoric and tinctorial strength in addition to their wide color range and good sublimation fastness. Moreover, azo disperse heterocyclic dyes are used for dyeing and silkscreen printing of textile fabrics [1-4]. Azo dyes have also been used as coloring agents for pharmaceutical targets to implement easy identification and imaging [5].

Sulfadiazine (SFD), sulfamerazine (SFMr), and sulfadimidine (SFDd) [6] are commonly referred in the pharmaceutical market as triple sulfa® drug for ophthalmic use because of their excellent antibacterial properties (Scheme 1). Moreover, the antimicrobial azo-sulfonamide drugs could be systemically employed for the chemotherapeutic treatments of bacterial infections in humans. There is a family of azo dyestuffs with a sulfonamide functional group that produces antimicrobial properties in the fibers. Prontosil®, the first member of these azo-sulfonamide antimicrobial drugs (Scheme 1), was introduced in 1932 as a promising medication against streptococcal infections in mice [7]. Prontosil showed its activity only *in vivo* mouse infection models with no apparent antibacterial efficacy against *Streptococci in vitro* [8]. This is due to the reductive cleavage of the azo bond of prontosil into their active component metabolites (sulfanilamide) inside the body. Sulfasalazine (SASP) is another antibacterial drug that consists of salicylic acid connected to the antibiotic sulfapyridine with azo linkage (Scheme 1) and was used for the treatment of rheumatoid arthritis (RA) symptoms [9]. On the other hand, thiopyrimidinone moiety was reported to have intrinsic antibacterial properties against different kinds of bacterial pathogens [10-14]. It has been affirmed that the thiopyrimidinone compounds inhibit the SecA protein essential for bacterial survival [15]. Spiropyrimidines, a class of pyrimidines connected with cyclic fragments through spiro carbon atom, has attracted many research groups due to their biological importance [16].

Recently, some research groups have been interested in the production of biologically and commercially important disperse dyes [17,18]. In fact, using azo dyes with a sulfonamide group (sulfonamide azo dyes) is a good technique to improve the light fastness of azo dyes on fibers [19]. Therefore, it is crucial to mix functional finishing and dyeing in one step by designing disperse dyes with an antibacterial moiety incorporated into the same molecule. Our goal is to design a scaffold consisting of the two antibacterial components (spirothiopyrimidine and sulfonamide)

*Corresponding author: she2rifx@yahoo.com
*Corresponding author: shaban_nrc@yahoo.com

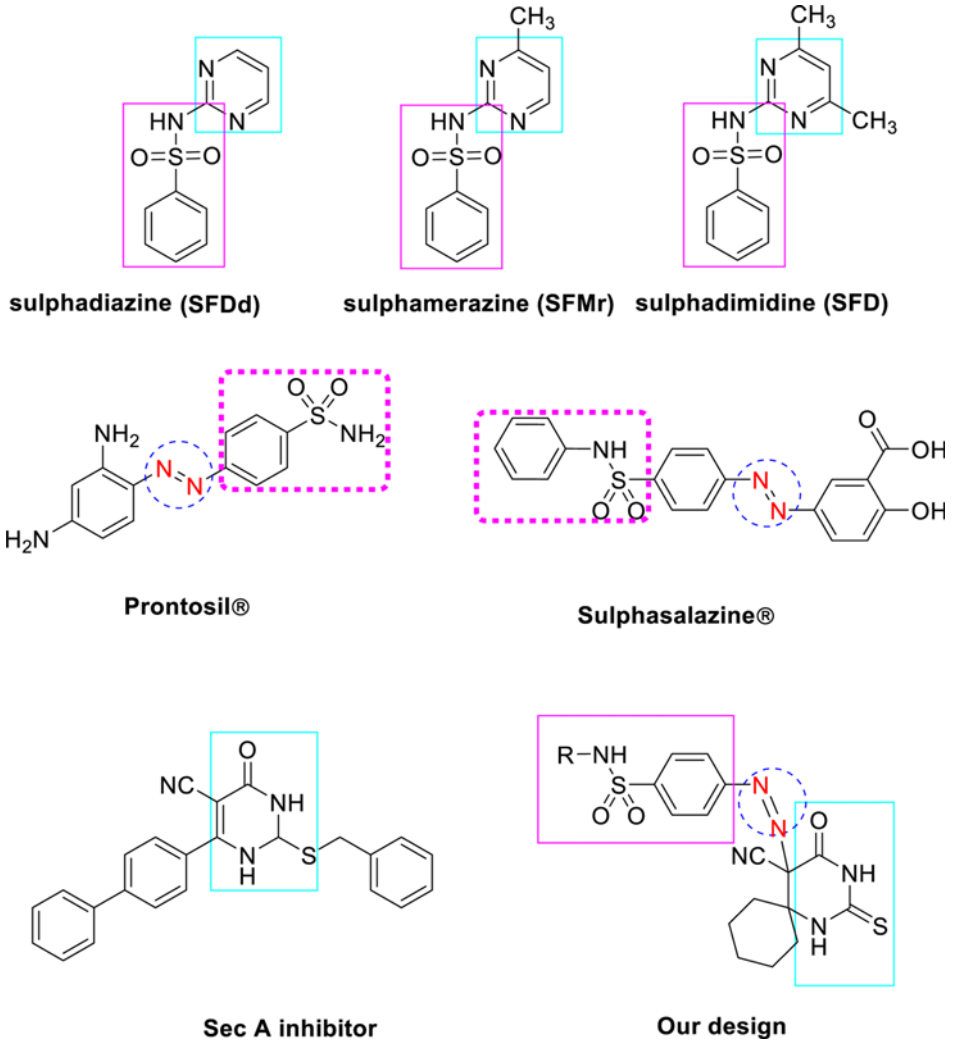

Scheme 1. Antibacterial drugs containing pyrimidine, sulfonamide, azo scaffolds.

connected with the cleavable azo linker as shown in Scheme 1.

In the current study, we report the first potential for the synthesis of bioconjugates containing spirocyclic thiopyrimdinone bridged to aryl/aryl sulfonamide with azo linker to investigate their applications as disperse dyes for polyester fabric printing as well as studying the antibacterial activity of both the dyes and the fabrics.

Experimental

Chemicals and Reagents

Sulfadiazine, aniline, *p*-chloroaniline, ethyl cyanoacetate, sodium nitrite, and potassium carbonate were supplied from Across Organic. Sulfanilamide was purchased from Fluka. Sulfapyridine and HCl were supplied from Sigma-Aldrich. Thiourea was purchased from Laboratory Rasayan, cyclohexanone was from BDH Chemicals Ltd., Poole, England, and DMF was from SDFCL. Ethanol (EtOH) (99 %), sodium dihydrogen phosphate (98.0 %), and sodium lignosulphonate (Anionic dispersing agent, Powder) (99.5 %) were bought from LOBAChemie. Sodium acetate (AcONa, 99 %) was obtained from East-Chem. Thickener (commercial synthetic thickener) acrylate copolymers and Lyprint (sodium salt of nitrobenzene sulfonic acid) were supplied from BASF Company. Polyester (150 g/m^2) were supplied by Egyptian and Developing Co., Cairo, Egypt. Daico thick 1600, a synthetic thickener for azo disperse silk screen-printing, was provided by Daico company.

Instruments and Methods

All ^{1}H- and ^{13}C-NMR spectra were recorded on a JEOL ECA500 FT NMR spectrometer at 500 MHz and 125 MHz, respectively, at Spectral Analyses Unit, National Research Center, Dokki, Egypt. Dimethyl sulfoxide (DMSO-d6) was used as a solvent. Chemical shifts were expressed in δ ppm

relative to the position respective to the solvent. Fourier transform infrared (FT-IR) spectra were recorded using a Thermo Fisher Nicolet IS10 at Spectral Analyses Unit, National Research Center, Dokki, Egypt. Electron impact ionization mass spectra (EI-MS) were obtained on a Thermos Scientific Trace 1310 Gas Chromatography-Mass Spectrometry at Cairo University, Egypt. UV/Vis absorption spectra for azo compounds were measured by a Hunter Lab Ultra Scan PRO spectrophotometer. The *in vitro* antibacterial screening was carried out at Micro Analytical Center, National Research Centre, Dokki, Egypt. Melting points (m.p.) were measured and recorded by a Stuart scientific melting point apparatus and were uncorrected. All synthesized products were detected by thin-layer chromatography (TLC) on Kiesel gel F254 precoated plates (Merck).

General Procedure for the Synthesis of Azospiropyrimidine Derivatives 4a-e

Under ice-cooling, an aqueous solution of $NaNO_2$ (0.34 g, 5.0 mmol) in the least amount of H_2O (2.0 m*l*) was dropwise added to the aryl amines **2a-e** (5.0 mmol) dissolved in conc. HCl (2.0 m*l*, 34 %), and the mixture was maintained cooled at 0-5 °C in an iced bath for an additional 30 min. The produced diazonium salt solution was added portion-wise to a separate Erlenmeyer flask containing a mixture solution of spiropyrimidine **1** (1.1 g, 5.0 mmol) and $AcONa{\cdot}3H_2O$ (1.02 g, 7.5 mmol) in 10 m*l* of EtOH-DMF (1/1), and the mixture was vigorously stirred in the iced bath at 0-5 °C for 3 h. The formed solid was filtered off under vacuum, washed three times with distilled water (3×10 m*l*), and one time with cold EtOH (1×10 m*l*), and air-dried to afford the pure azo compounds **4a-e** in excellent yields.

4-Oxo-2-Thioxo-1,3-Diazaspiro[5.5]Undecane-5-Carbonitrile (1)

Pale yellow crystals; m.p. 230-232 °C: lit. m.p. 228-230 °C [20]. ^{1}H-NMR (500 MHz, DMSO-d6): δ=1.10-1.90 (m, 10 H, 5 CH_2), 4.70 (s, 1 H, CH), 9.95 (s, 1 H, NH), 12.05 (s, 1 H, NH) ppm.

(E)-4-Oxo-5-(Phenyldiazenyl)-2-Thioxo-1,3-Diazaspiro [5.5]Undecane-5-Carbonitrile (4a, $C_{16}H_{17}N_5OS$)

Pale yellow crystals; m.p.113-115 °C; IR (KBr): ν=3314 (NH), 3104 (NH), 2941 (CH aliph.), 1723 (C=O) cm^{-1}; ^{1}H-NMR (500 MHz, DMSO-d6): δ=1.52-1.96 (m, 10 H, 5 CH_2), 7.53-7.62 (t, 2 H, J=10 Hz, Ar-H), 7.63-7.69 (t, 1 H, J=10 Hz, Ar-H), 7.70-7.75 (d, 2 H, J=10 Hz, Ar-H) 10.20 (s, 1 H, NH), 12.33 (s, 1 H, NH) ppm; ^{13}C-NMR (125 MHz, DMSO-d6): δ=20.50, 20.96, 24.68, 30.04, 31.60, 61.36, 82.73, 112.68, 123.71, 130.32, 134.06, 150.79, 158.67, 177.49 ppm; MS (EI): m/z (%)=327 (12) [M$^+$].

(E)-5-((4-Chlorophenyl)Diazenyl)-4-Oxo-2-Thioxo-1,3-Diazaspiro[5.5]Undecane-5-Carbonitrile (4b, $C_{16}H_{16}ClN_5OS$)

Pale yellow crystals; m.p.: 182-184 °C; IR (KBr): ν=3.316 (NH), 3.124 (NH), 2.937 (CH aliph.), 1,721 (C=O) cm^{-1}; ^{1}H-NMR (500 MHz, DMSO-d6): δ=1.47-1.93 (m, 10 H, 5 CH_2), 7.60-7.77 (d, 2 H, J=5 Hz, Ar-H), 7.73-7.81 (d, 2 H, J=10 Hz, Ar-H), 7.70-7.75 (d, 2 H, J=10 Hz, Ar-H) 10.18 (s, 1 H, NH), 12.33 (s, 1 H, NH) ppm; ^{13}C-NMR (125 MHz, DMSO-d6): δ=20.53, 20.94, 24.65, 30.06, 31.57, 60.97, 81.85, 112.67, 124.99, 130.70, 138.48, 148.82, 158.18, 177.87 ppm; MS (EI): m/z (%)=361 (18) [M$^+$].

(E)-4-((5-Cyano-4-Oxo-2-Thioxo-1,3-Diazaspiro[5.5] Undecan-5-yl)Diazenyl)Benzenesulfon-Amide (4c, $C_{16}H_{18}N_6O_3S_2$)

Pale yellow crystals; m.p.: 182-184 °C; IR (KBr): ν=3.326 (NH), 3.287 (NH_2), 3.100 (NH), 2.940 (CH aliph.), 1.722 (C=O) cm^{-1}; ^{1}H-NMR (500 MHz, DMSO-d6): d=1.54-2.06 (m, 10 H, 5 CH_2), 7.61 (s, 2H, NH_2), 7.87-7.94 (d, 2 H, J=10 Hz, Ar-H), 8.0-8.10 (d, 2 H, J=10 Hz, Ar-H), 10.22 (s, 1 H, NH), 12.38 (s, 1 H, NH) ppm; ^{13}C-NMR (125 MHz, DMSO-d6): d=20.59, 20.91, 24.61, 30.10, 31.51, 61.36, 82.74, 112.68, 124.18, 127.88, 148.33, 152.07, 158.67, 177.48 ppm; MS (EI): m/z (%)=406.08 (15) [M$^+$].

(E)-4-((5-Cyano-4-Oxo-2-Thioxo-1,3-Diazaspiro[5.5] Undecan-5-Yl)Diazenyl)-N-(Pyridin-2-yl)Benzenesulfonamide (4d, $C_{21}H_{21}N_7O_3S_2$)

Pale yellow crystals; m.p.: 165-168 °C; IR (KBr): ν=3.314 (NH), 3.194 (NH), 2.937 (CH aliph.), 1.718 (C=O) cm^{-1}; ^{1}H-NMR (500 MHz, DMSO-d6): δ=1.37-1.98 (m, 10 H, 5 CH_2), 6.78-6.85 (t, 1 H, J=5 Hz, Het-H), 7.16-7.25 (d, 1 H, J=10 Hz, Het-H), 7.71-7.79 (t, 1 H, J=10 Hz, Pyr-H), 7.82-7.88 (d, 2 H, J=5 Hz, Ar-H), 7.90-7.95 (d, 1 H, J=5 Hz, Het-H), 8.0-8.1 (d, 2H, J=5 Hz, Ar-H), 10.19 (s, 1 H, NH), 12.37 (s, 1 H, NH), 12.8 (brs, 1 H, NH) ppm; ^{13}C-NMR (125 MHz, DMSO-d6): δ=20.55, 20.90, 24.59, 30.05, 31.52, 61.38, 82.98, 99.97, 112.75, 115.38, 124.10, 128.63, 142.22, 151.668, 154.54, 158.18, 177.48 ppm; MS (EI): m/z (%)=483.11 (8) [M$^+$].

(E)-4-((5-Cyano-4-Oxo-2-Thioxo-1,3-Diazaspiro[5.5] Undecan-5-yl)Diazenyl)-N-(Pyrimidin-2-yl)Benzenesulfonamide (4e, $C_{20}H_{20}N_8O_3S_2$)

Pale yellow crystals; m.p.: 165-168 °C; IR (KBr): ν=3.404 (NH), 3,097 (NH), 3037 (NH_2), 2,948 (CH aliph.), 1,720 (C=O) cm^{-1}; ^{1}H-NMR (500 MHz, DMSO-d6): δ=1.53-1.98 (m, 10 H, 5 CH_2), 6.99-7.05 (t, 1 H, J=5 Hz, Het-H), 7.85-7.93 (d, 2 H, J=10 Hz, Ar-H), 8.13-8.21 (d, 2 H, J=10 Hz, Ar-H), 8.46-8.52 (d, 2H, J=5 Hz, Het-H), 10.22 (s, 1 H, NH), 12.23 (brs, 1 H, NH), 12.40 (s, 1 H, NH) ppm; ^{13}C-NMR (125 MHz, DMSO-d6): δ=20.57, 20.89, 21.56, 24.58, 30.08, 31.49, 34.22, 61.36, 82.95, 112.76, 113.57, 116.08, 116.26, 123.87, 129.77, 129.95, 144.96, 152.44, 157.13, 158.28, 158.83, 177.77 ppm; MS (EI): m/z (%)=484.11 (5) [M$^+$].

Preparation of Printing Paste

The proportions utilized to make the components of the printing paste are shown in Table 1. The printing paste was used for silkscreen printing of polyester fabrics samples according to the conventional screen-printing method. The prints were then dried at room temperature before being thermo-fixation for 4 min at 180 °C. The prints were washed

Table 1. Proportions utilized to make the components of the printing paste

Dye	2 g
Thickener	75 g
Lyprint	3 g
Sodium dihydrogen phosphate	5 g
Sodium lignosulfonate	1 g
Water	X
Total	100 g

twice in cold water, then twice in hot water, then again in cold water, before being soaped at 60 °C for 30 min with 2 g/*l* nonionic detergent and finally air-dried.

Color Measurements

The colorimetric strength data were then measured upon soaping of the printed polyester fabric samples by light reflectance technique using a Hunter Lab Ultra Scan PRO spectrophotometer, as the results were shown in Table 2. The soaping of the printed samples assumes that the *K/S* values are proportionate to the dye concentration on the fiber under the printing conditions used, at least at the concentration of dyes used (2.0 g in the paste). Using the Kubelka-Munk (equation (1)), the color strength was determined as *K/S*.

$$K/S = \frac{(1-R)^2}{2R} \quad (1)$$

where *R*=decimal fraction of the dyed fabric reflection, *K*= absorption coefficient, and *S*=scattering coefficient.

Fastness Properties Methods

The fastness properties of the printed samples were tested using standard ISO methods [21-25]. These properties included rubbing, washing, perspiration, light, and sublimation. While the washing fastness was evaluated using the ISO 105-C06 B2S [21] standard technique (4.0 g/*l* ECE detergent, 1.0 g/*l* sodium perborate, 25 steel balls) at 60 °C for 30 min and a liquor ratio of 50:1. The ISO 105X12 rubbing fastness test [25] and the ISO 105-E04 perspiration fastness test [22] were also tested. The fixometer was used to perform the sublimation fastness test at 180 and 210 °C in agreement with ISO 105P01 [26]. A xenon arc lamp test was used to determine light fastness in accordance with ISO 105-B02 [24]. For the rubbing fastness study, the specimens measuring 5 cm×5 cm were cut and put on the crock meter's bed. Then, a 5 cm×5 cm white-bleached sample was put on the finger of the crock meters and rubbed against the sample fabric for 10 s and 10 cycles. The ISO 105X12 techniques [26] was used to test the color fastness to rubbing (both wet and dry). For the sublimation fastness, an iron tester (Yasuda No. 138) was used, and the dye-printed sample was sandwiched between two pieces of cotton and polyester fabric that had not been colored. All samples should be the same diameter and treated for 1 min at 180 °C and 210 °C.

Determination of Antibacterial Activity

Pathogenic Strains

Bacillus cereus B-3711 was obtained from the Northern Regional Research Laboratory in Illinois, USA (NRRL), *Listeria monocytogenes* 598 was obtained from the Food Science department at Massachusetts University in the United States, and *Escherichia coli* 0157:H7, *Salmonella typhmirum*, and *Staphylococcus aureus* were isolated from serologically identified bacteria at the National Research Center's Dairy Microbiological Laboratory.

In Vitro Antimicrobial Screening

The inhibition zones diameters were estimated by disc diffusion according to Tamokou method [27] with some modifications. Antibacterial stock solutions (concentration of 1 mg/m*l*.) of the five synthesized dyes **4a-e** were prepared. For antibacterial (10 μg/disk): sterile discs were soaked in 10 μ*l* of each compound; a control was loaded with 10 μ*l* of DMSO. The discs of the loaded compounds were placed on the inoculated plat surface using sterile forceps. The five compounds were tested for antimicrobial activity against some human pathogenic microorganisms: Gram (+) bacteria (*S. aureus*, *L. monocytogenes*, and *B. cereus*), Gram (-) bacteria (*S. typhmirum* and *E. coli*). Cefoperazone was used as a positive control for bacteria (100 μg/m*l*), while DMSO solution (10 % v/v) was used as the negative control. Within 15 min, and after the discs were applied, the bacterial plates were incubated at (37 °C-18 h). The bacterial inhibition zones were assessed for growth inhibition using sliding calipers.

Antimicrobial Assessment of the Dyed Fabrics

The dyed fabrics were subjected to investigate their antimicrobial activity against Gram (-ve) and Gram (+ve) bacteria using the AATCC test method 100-1999 to detect bacteriostatic and antibacterial activities of the diffusible antimicrobial agents on treated textile materials toward two different types of bacterial strains. Following this method, fabric swatches (about 36 mg) of the dyed fabrics encoded **4a-e** were confronted with 36 μ*l* of bacterial inoculums (10^5 CFU of bacteria). The inoculated fabric samples were immersed in 10 m*l* of sterilized water for 5 h as a contact time. After the time was calculated, 40 μ*l* of sterilized water was placed onto nutritional agar and then incubated for eighteen hours at 37 °C. Counting of the viable bacteria colonies on the agar plate, and the percentage reduction in bacteria counts was measured using:

$$R\% = ((B - A)/B) \times 100$$

where *R*=the bacterium reduction percentage, while *A*, *B*=bacterial colonies number on treated and untreated fabrics, respectively.

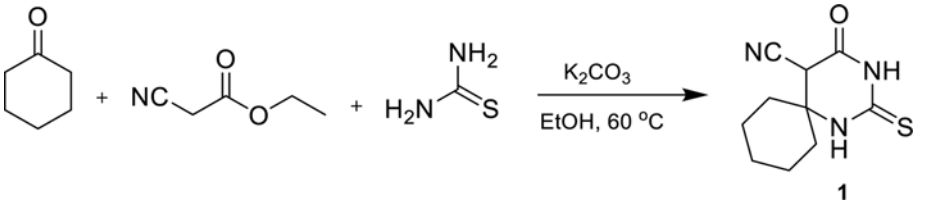

Scheme 2. Synthesis of spirocyclohexyl 2-thiopyrimidinone **1**.

Results and Discussion

Chemistry

Synthesis and Structural Characterization

In the current study, we designed novel conjugates combining spirocyclic 2-thiouracil and aryl sulfonamide moieties through azo bridge to develop innovative heterocyclic azo-disperse dyes. Furthermore, we studied the applications of these azo dyes in textile printing and investigated the antibacterial activity of the dyes as well as their fabrics. The target molecules were simply obtained on a gram scale via exploiting, for the first time, the active methine center of the spirocyclic 2-thiopyrimidinone **1** for diazocoupling with aryl diazonium chloride derivatives **3a-e** to furnish the heterocyclic azo-disperse dyes **4a-e** in excellent yield. The synthetic approaches for starting compound or the azo dye conjugates are outlined in the schemes below. The starting 1,3-diazaspiro[5.5]undecane **1** was prepared according to the synthetic protocol [20] by two different methods, either through the application of ultrasound irradiation conditions or the conventional methods for the one-pot reaction of cyclohexanone, ethyl cyanoacetate, and thiourea in EtOH using K_2CO_3 as a basic catalyst to deliver the spiro-5-cyanopyrimidine **1** in good yield (Scheme 2).

The reaction pathway for the formation of azo compounds **4a-e** included three steps as shown in Scheme 3. The first step involves the generation of the anionic intermediate **A** via proton abstraction from the active methine group in spiropyrimidine **1** by the basic aid of AcONa. The second step includes the diazotization of aryl amines **2a-e** with conc. HCl and $NaNO_2$ solution at 0-5 °C to generate the corresponding aryl diazonium chloride **3**. Finally, the reaction ends with the coupling of the electrophilic diazonium salt **3** with the nucleophilic spiropyrimidine anion **A** under basic conditions to afford the required azo-dye products **4a-e** in excellent yields as depicted in Scheme 3.

The structures of compounds **4a-e** were assigned based on the spectral analysis. Specifically, the FT-IR spectra of **4a-e** showed the characteristic bands of (NH and NH_2 stretching) ranging from 3400 to 3000 cm^{-1}, while the >C=O stretching of **4a-e** is evident from the appearance of the corresponding absorption band around 1720 cm^{-1}. Furthermore, the development of absorption bands ranging from 1550 to 1470 cm^{-1} is assigned to the azo (-N=N-) group. The ^{1}H-

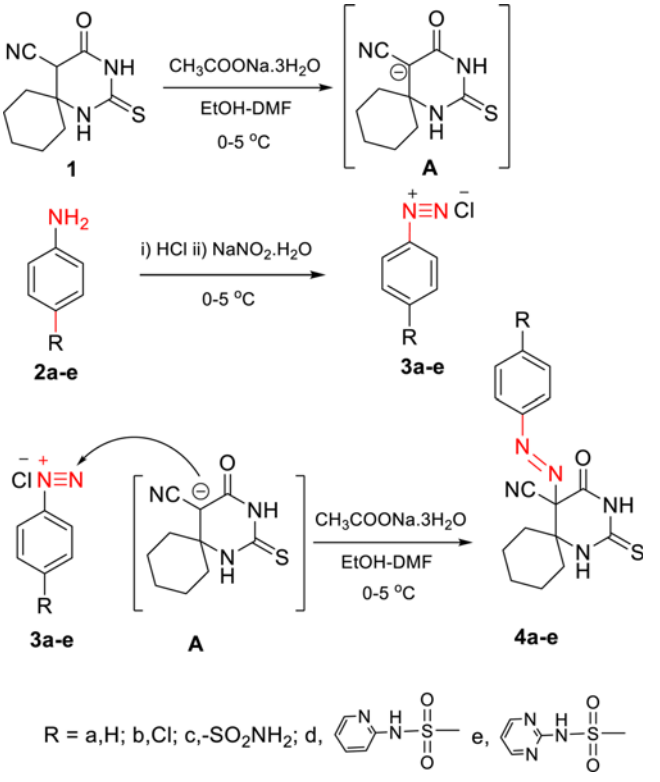

Scheme 3. Synthesis Azo dye derivatives **4a-e**.

NMR displayed multiplet peaks at 1.54-1.99 ppm which correspond to the spirocyclohexyl protons, and the NH protons of the thiouracil ring appeared as two singlet peaks around 10.0, 12.0 ppm, while the corresponding methine proton (-CH-) that was existed at 4.7 ppm in the ^{1}H-NMR spectrum of the starting compound **1** is absent in the spectra of the products and this finding established that the azo coupling occurred at this site. Additionally, the aromatic and heterocyclic protons are displayed in the spectra at the region 7.0-8.5 ppm. The ^{13}C-NMR of **4a-e** showed the characteristic signal of the quaternary spiro carbon at 61.0 ppm, while the -C≡N has typically appeared at 112.0 ppm. Moreover, the >C=O and >C=S carbons resonated at 159.0 and 177.0 ppm, respectively. Finally, the mass spectral analysis exhibited the molecular ion peaks with expected values, which unambiguously confirmed the chemical

Table 2. Printed azo disperse dyes samples were evaluated in terms of color

Dye	Color shade	Absorption [λ_{max}(nm)]	*K/S*	L^*	a^*	b^*	C^*	*h*
4a	Yellow	375	7.18	13.94	33.46	69.91	83.28	26.02
4b	Yellow	375	12.77	13.44	23.43	75.08	91.14	19.07
4c	Yellow	380	12.48	24.07	13.71	77.74	102.99	12.32
4d	Orange yellow	425	13.66	27.75	46.99	62.47	69.30	37.00
4e	Orange yellow	390	14.19	27.03	42.90	59.06	67.20	37.21

where *K/S*=color strength, L^*=lightness, a^*=degree of redness, b^*=degree of yellowness, c^*=chroma, *h*=hue.

structure of **4a-e**.

Textile Printing

The novel heterocyclic disperse azo dyes were synthesized from a spirocyclic 2-thiopyrimidine hybrid with sulfonamide moieties and employed in the production of pastes for printing polyester fabrics.

Color Strength Measurements (*K/S*) and Analyses

Table 2 shows the color intensity of screen-printed dyes applied to PE expressed as *K/S*, as well as the color shades of dyed fabrics. The chemical structure and kind of substituent on the aromatic moiety of produced dye have an evident influence on the value of the *K/S* values, which make varied prints values. The color strength of dyes **4e**, **4c**, **4d** was higher, and the outcomes were better compared to dyes **4a**, **4b**. This could be due to the increased conjugation of the benzenesulfonamide coupling component. The dye **4d** has higher absorption than that of the dyes **4a**, **4c**, which leads to increased dye dispersion and build-up on the fiber. The lightness (L^*) of the azo compounds **4a** and **4b** is lower than that of **4d**, **4e**, **4c**. Using the following equations [28,29], the hue angle (*h*°) and chroma (saturation) (c^*) were calculated:

$$c^* = \sqrt{(a^*)^2 + (b^*)^2} \quad (2)$$

$$h = \tan^{-1}\left(\frac{a^*}{b^*}\right) \quad (3)$$

The positive values of a^* and b^* changed the color hues of the dyes on the polyester fabric towards the reddish-yellowish direction.

Fastness

Washing Fastness

The property of colored fabrics to retain their color after being washed with detergents and soaps is known as wash fastness. The color fastness to washing was determined using the ISO 105-C06 B2S technique [28]. The standard greyscale (Table 3) is used to detect staining on adjacent white fabrics and color changes in dyed samples (1=poor, 2=moderate, 3=good, 4=very good, 5=excellent). The movement rate of prepared dyes out of polyester fabric during washing was used to determine the washing fastness properties, based on different parameters such as water solubility, the nature of the mechanical link between the dye and the fibers, the dye's molecular size, and the nature as well as the location of the charge on both the dye molecules and the fabrics. The polyester fabric printed with dyes **4d** and **4e** yielded very good to excellent (4-5) results. Because **4e** and **4d** are larger in size, they will be confined inside the polyester fabric inter-polymer chain space, increasing hydrophobicity by increasing aromatic rings [30,31].

Perspiration Fastness

The perspiration fastness data (in basic and acidic solutions) shown in Table 3 shows that the molecular weight of the dye and the attraction binding force between the azo dispersion dye and the fabric affect the dye removal from the surface of polyester fabric. The polyester fabric printed with dyes **4d** and **4e** provided very good to excellent (4-5) results (Table 3). It is clear that there is an inverse correlation

Table 3. Polyester fabric printed with dyes **4a-e** exhibits good fastness properties

Sample	Light fastness	Washing fastness[a)]		Rubbing		Perspiration fastness[a)]	
		St alt		Wet dry		St alt	
4a	6	3-4	2-3	2-3	3-4	2-3	2-3
4b	7	3-4	3-4	4-5	4-5	2-3	3-4
4c	6	4-5	3-4	3-4	4-5	3-4	2-3
4d	7	4-5	4-5	3-4	3-4	4-5	4-5
4e	7	4-5	4-5	3-4	3-4	4-5	3-4

[a)]Alt is an alteration in color and St is a staining on cotton.

Table 4. Sublimation fastness properties of the polyester fabric printed with dyes **4a-e**

Sample	Sublimation fastness at 180 °C	Sublimation fastness at 210 °C	Staining on fabric after sublimation polyester	Staining on fabric after sublimation cotton
4a	3-4	3-4	3-4	2-3
4b	3-4	3-4	3-4	2-3
4c	4	3-4	4	3-4
4d	4-5	4-5	4-5	3-4
4e	4-5	4-5	4-5	3-4

between the dye removal rate and the molecular weight of the dye [32].

Rubbing Fastness

The removal of loosely located or attached dye structure from the surface of the printed polyester fabric is indicated in Table 3. The goal of this test (both wet and dry) is to determine how much color is transferred by rubbing from the surface of colored fabrics to another undyed fabric surface. Most of our dyes have excellent rubbing fatness, which can be attributed to adequate dye molecule diffusion into the fabrics and may be also due to the higher dye fixation on the fiber. The conventional greyscale (1 to 5) was used with one being the lowest and five being the highest.

Light Fastness

The ISO 105-B02 technique [24] was used to determine the color fastness to light. The nature of the substituents, which change the electron density surrounding the azo group, has a substantial impact on the light fastness. Electron withdrawing groups may be responsible for the high light fastness. Thus the azo compounds with this kind of substituents are less photosensitive. Generally, all the prepared azo disperse dyes **4a-e** showed satisfactory fastness to light (6-7), as noticed from Table 4.

Fastness to Sublimation

The sublimation fastness results are shown in Table 4. The heat treatment is correlated with the migration of azo disperse dyes off the surface of polyester fabric. The undyed polyester-cotton fabrics employed for the sublimation fastness tests had typically good results that matched the international geometric grayscale [23]. The polarity of the substituent groups, such as the presence of SO_2NH groups in all dyes, may contribute to the good sublimation fastness results [33].

Antimicrobial Assay

The *in vitro* antimicrobial properties of the dyes encoded **4a-e** were investigated against *S. aureus* and *B. subtilis* as Gram (+ve) bacteria and *E. coli*, *S. typhmirum,* and *L. monocytogenes* as Gram (-ve) bacteria using the disc paper diffusion technique (Table 5). To illustrate the efficacy of synthesized dyes, antibacterial tests were performed in contrast to the cefoperazone drug. The results assigned that the produced dyes had different activity depending on the microbial strains examined. For example, compound **4d** was the most active substance from the test samples against the Gram (+ve) bacteria (*S. aureus*) (15 mm) and had higher activity than the reference drug cefoperazone (11 mm). Furthermore, when compared to other compounds, its antibacterial activity was highly active against Gram (-ve) bacteria (*E. coli*), with an inhibition zone of 14.5 mm (Table 5).

On the other hand, all the synthesized dyes showed a high inhibition zone (12-14.5 mm) (Figure 1) against *B. cerus*, and satisfactory activity against *S. typhmirum* ranged from (9.5 to 11.25 mm). However, a different trend in antibacterial activity against *L. monocytogenes* was observed with all dyes that were inactive against it except 4b that showed a satisfactory activity against *L. monocytogenes* with an inhibition zone (9 mm). The antibacterial activity of the

Table 5. Antibacterial evaluation of produced dyes **4a-e** against Gram (+ve) and Gram (-ve) bacteria in terms of bacterial inhibition zone diameter at 1 mg/m*l* concentration

Compounds (1 mg/m*l*)	Test microorganisms				
	Gram (+ve) bacteria			Gram (-ve) bacteria	
	S. aureus	*B. cereus*	*E. coli*	*S. typhmirum*	*L. monocytegenes*
4a	15	13.5±2.1	11.5±0.7	11.25±0.3	-
4b	11.75±0.35	14.5±2.1	11.25±0.3	9.5±0.7	9
4c	12.5±0.7	12	11	10.5±0.7	-
4d	15.5±0.7	14±1.4	14.5±0.7	9.5±0.7	7
4e	12.5±3.5	14.5±0.7	10.5±0.7	11	7
Cefoperazone (100 μg/m*l*)	11	12.5±0.7	12.75±0.3	13.5±0.3	12

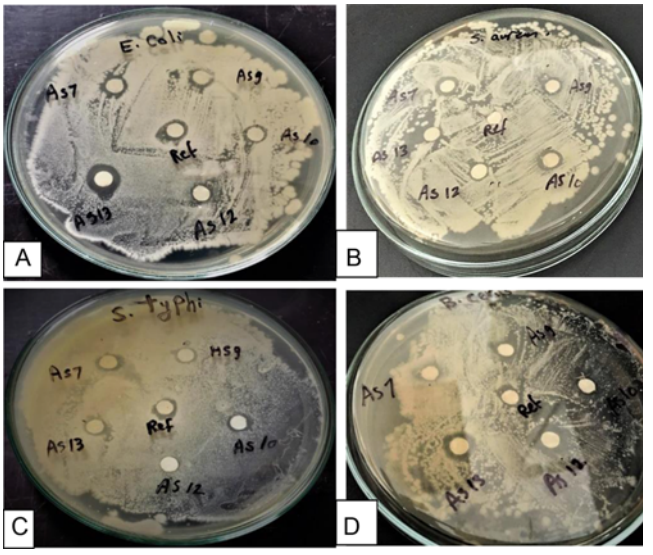

Figure 1. Antimicrobial effect of the dyes (**4a-e**) on the following; (A) *E. coli*, (B) *S. aureus*, (C) *S. typhmirum*, and (D) *B. cerus.*

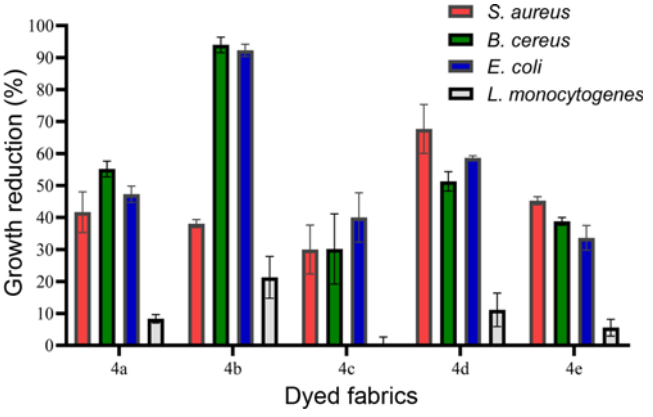

Figure 2. Antimicrobial efficacy of dyed fabrics according to the AATCC 100-1999 method; bacteria concentrations: 10^5 CFU/m*l*; contact time: 18 h.

treated fabrics was also investigated using the AATC 100-1999 method. The results shown in (Figure 2) revealed that the dyed fabrics offer varying degrees of inhibition against the tested bacteria.

The antimicrobial data indicated that the dyed fabric with (**4b**) has a strong inhibition on *B cereus* (93 %) within 18 h of contact time (Figure 3(A)). Surprisingly, among all dyed fabrics, the fabric dyed with **4b** also displayed potent antimicrobial activity against *E. coli* with a reduction of more than 90 % (Figure 3(B)). On the other hand, the negative control had no inhibitory impact on any of the bacteria tested. Furthermore, **4d**-dyed fabrics were able to kill approximately 63 % of *S. aureus* and 58 % of *E. coli* germs within the contact time. However, for the dyed fabric **4a**, no growth inhibition against *S. typhmirum* under the

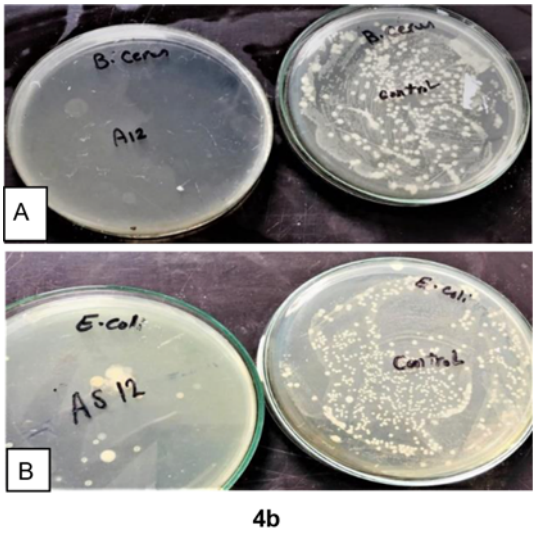

Figure 3. Antimicrobial activity of the dyed fabrics (**4b**) and untreated fabric (control) by the AATCC 100-1999 standard method against; (A) *B. cerus* and (B) *E. coli.*

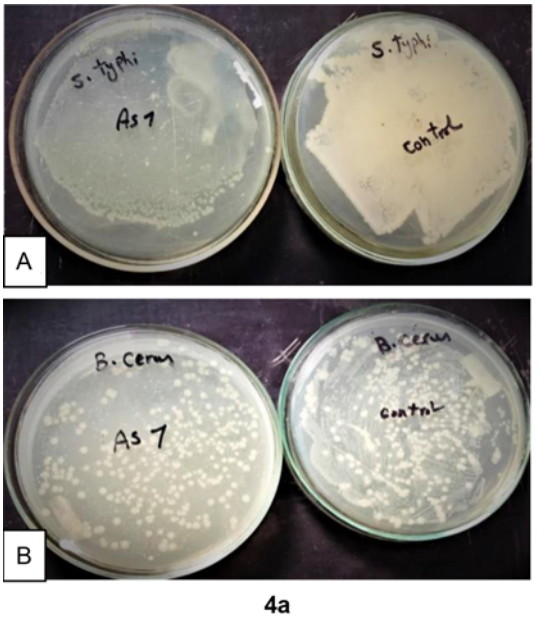

Figure 4. Antimicrobial activity of the dyed fabrics (**4a**) and untreated fabric (control) by the AATCC 100-1999 standard method against; (A) *S. typhmirum* and (B) *B. cerus*.

fabric was observed when AATCC 147 was used (data not shown), but it was less crowded compared to the untreated fabric (Figure 4(A)).

It is evident that the antibacterial activity differs among the evaluated dyes and fabrics due to differences in the cell walls of the bacteria tested and their susceptibility to antimicrobial agents. The interest in a specific antimicrobial azo sulfonamide dye depends on the type of antimicrobial

activity evaluation and the microorganism population. The involvement of 4-amino benzoic acid in the folic acid pathway to block foliate synthase is key to the antibacterial mechanism of functional dyestuffs such azo sulfonamides. In this regard, sulfonamide inhibits folic acid synthesis in bacteria, and in turn, limits purine biosynthesis accordingly [33,34]. The biological activity of azo sulfonamide antibiotics is associated to their 4-aminophenyl sulfonamide core, which can feature various substituents at the sulfonamide nitrogen. The current results provides implications for the development of effective azo sulfonamide dyes with high antibacterial activity against antibiotic-resistant microorganisms.

Conclusion

The development, production, and characterization of a new class of azo dyes having a sulfonamide chromophore have been implemented. The new synthetic dyes were used for silkscreen printing of polyester fabrics. In terms of washing, perspiration, rubbing, and light fastness, the color measurements and fastness properties of the dyes produced ranged from moderate to high. In addition, the good antibacterial activity of the synthesized dyes should lead to the development of new antimicrobial azo disperse dyes with improved application features.

Conflict of Interest

The authors declare that there is no conflict of interest.

Electronic Supplementary Material (ESM) The online version of this article (doi: 10.1007/s12221-022-4032-4) contains supplementary material, which is available to authorized users.

References

1. G. M. Malik and S. K. Zadafiya, *Chem. Sin.*, **1**, 15 (2010).
2. G. A. M. Nawwar, K. S. A. Zaher, E. Shaban, and N. M. A. El-Ebiary, *Fiber. Polym.*, **21**, 1293 (2020).
3. E. Shaban, S. H. Nassar, S. Shabban, and H. E. Gaffer, *Egypt. J. Chem.*, **60**, 73 (2017).
4. K. M. Hassan, S. A. S. ElKhabiery, G. M. ElHaddad, S. H. Shokair, and I. E. ElSayed, *J. Iran. Chem. Soc.*, **19**, 147 (2022).
5. A. Gičević, L. Hindija, and A. Karačić, "International Conference on Medical and Biological Engineering", pp.581-587, doi: 10.1007/978-3-030-17971-7_88, 2019.
6. J. Mokhtari, A. Shams-Nateri, and P. Ferdosi, *Fiber. Polym.*, **15**, 1369 (2014).
7. R. Bentley, *J. Ind. Microbiol. Biotechnol.*, **36**, 775 (2009).
8. Y. Guo, H. Lee, and H. Jeong, *Prog. Mol. Biol. Transl. Sci.*, **171**, 61 (2020).
9. G. Plosker and K. Croom, *Drugs*, **65**, 2591 (2005).
10. N. Sala, G. Prats, M. Villabona, I. Gallardo, T. Hamdan, R. O. Al-Kaysi, J. Hernando, and G. Guirado, *Dyes Pigm.*, **153**, 160 (2018).
11. P. Cui, X. Li, M. Zhu, B. Wang, J. Liu, and H. Chen, *Eur. J. Med. Chem.*, **127**, 159 (2017).
12. A. S. Chaudhary, J. Jin, W. Chen, P. C. Tai, and B. Wang, *Bioorg. Med. Chem.*, **23**, 105 (2015).
13. M. S. Mohamed, S. M. Awad, and N. M. Ahmed, *Acta Pharm.*, **61**, 171 (2011).
14. K. Cheng, Q.-Z. Zheng, Y. Qian, L. Shi, J. Zhao, and H.-L. Zhu, *Bioorg. Med. Chem.*, **17**, 7861 (2009).
15. A.-A. S. El-Etrawy and F. F. Sherbiny, *J. Mol. Struct.*, **1232**, 129993 (2021).
16. A. S. Chaudhary, W. Chen, J. Jin, P. C. Tai, and B. Wang, *Future Med. Chem.*, **7**, 989 (2015).
17. R. M. Abd El-Aal and M. Younis, *Dyes Pigm.*, **60**, 205 (2004).
18. M. Ma, Y. Sun, and G. Sun, *Dyes Pigm.*, **58**, 27 (2003).
19. P. Sah, J. Oneto, and H. Sah, *Arzneimittel-Forschung*, **10**, 533 (1960).
20. E. M. Hussein, *Monatsh. Chem.*, **144**, 1691 (2013).
21. TS EN ISO, "Textiles-Tests for Colour Fastness-Part C06: Color Fastness to Domestic and Commercial Laundering (TS EN ISO 105-C06)", 2012.
22. ISO 105-E04:2008, "Textiles - Tests For Colour Fastness - Part E04: Colour Fastness to Perspiration", 2008.
23. U. Nimkar and R. Bhajekar, *Colorage*, **43**, 135 (2006).
24. ISO 105-B02:2013, "Textiles - Tests for Colour Fastness - Part B02: Colour Fastness to Artificial Light: Xenon Arc Fading Lamp Test", 2013.
25. ISO 105-X12:2001, "Textiles - Tests for Colour Fastness - Part X12: Color Fastness to Rubbing", 2001.
26. B.S 1006:1990, "Standard Methods for the Determination of the Colour Fastness of Textiles and Leather", 5th eds., 1991.
27. J. Tamokou, A. Mbaveng, and V. Kuete in "Medicinal Spices and Vegetables from Africa" (V. Kuete Ed.), p.207, Elsevier, 2017.
28. J. M. Jabar, A. I. Ogunmokun, and T. A. A. Taleat, *Fash. Text.*, **7**, 1 (2020).
29. M. R. Luo, "Encyclopedia of Color Science and Technology", Springer, New York, NY, 2016.
30. M. Sadeghi-Kiakhani and S. Safapour, *Color. Technol.*, **131**, 142 (2015).
31. S. M. Al-Mousawi, M. A. El-Apasery, and M. H. Elnagdi, *Molecules*, **18**, 11033 (2013).
32. Y. M. Elkholy, M. H. Helal, and A. W. Erian, *Pigment Resin Technol.*, **30**, 168 (2001).
33. P. J. Shah, H. S. Patel, and B. P. Patel, *J. Saudi Chem. Soc.*, **17**, 307 (2013).
34. T. D. Brock, M. T. Madigan, J. M. Martinko, and J. Parker, "Brock Biology of Microorganisms", Pearson Prentice-Hall, Upper Saddle River, NJ, 2003.